3/17/92

LOCAL ADAPTIVE GRID REFINEMENT (LAGR) FOR CONTAMINANT TRANSPORT MODELING

Andrew V. Wolfsberg and David L. Freyberg

Department of Civil Engineering
Stanford University
Stanford, CA 94305-4020

Abstract

The success of a groundwater contaminant transport model is dependent on: 1) how well the relevant physical, chemical, and microbiological processes controlling subsurface transport are represented with mathematical equations and their parameters, and 2) how accurately and efficiently the equations are solved. For reactive, multicomponent problems in two or more dimensions, the computational burden of meeting the second goal becomes increasingly difficult as the complexity of the problem formulation required to meet the first goal increases. To address these two goals, we have implemented a system of local adaptive grid refinement (LAGR) to achieve efficient and accurate computational results for multidimensional, multicomponent transport problems. LAGR is based on automatic generation of multiple, high resolution patch grids (finite difference in this case) placed at locations in the solution domain where necessary to achieve uniform solution accuracy.

We have applied LAGR to nonreactive single component problems and to reactive multicomponent problems including such chemical processes as competitive sorption. As with familiar single component benchmark problems, numerical errors such as peak clipping, oscillations, and over- and undershoot plague the coarse grid computations for our multicomponent problems. In fact, these problems are exaggerated in some multicomponent problems because the fronts are sharper as a result of the interactive chemistry. Accurate solutions to these problems are provided using LAGR at a fraction of the computational cost of using a uniform fine grid.

1 Introduction

Accuracy and efficiency are two considerations which challenge any successful groundwater solute transport model. One condition for accuracy is that the relevant physical, chemical, and microbiological processes controlling subsurface transport be represented with appropriate mathematical equations. A second condition for accuracy is that the equations be solved with as little error as possible. Meeting both of these goals, and doing so efficiently, becomes increasingly more challenging as the number of governing processes, as well as the size and dimension of the problem formulation, increase.

One of the primary difficulties in computing accurate solutions to solute transport equations with numerical methods is overcoming such numerical errors as oscillations, over- and undershoot, and peak clipping. These errors are generally a result of insufficient numerical resolution in regions where the concentration gradient is changing rapidly. One way to overcome these errors is to supply uniformly high resolution over the entire solution domain. However, because the regions affiliated with the numerical error tend to propagate across the solution domain, such an approach is inefficient. For multicomponent problems with chemical and biological reactions, the computational burden per time step at each computational node may be hundreds of times greater than for non-reactive single species problems. The cost of supplying high nodal resolution uniformly over the entire solution domain for such problems makes accurate, field-scale computations difficult, if not unattainable.

In this paper, we present a method which enhances the efficiency in achieving accurate solutions for complex problems described by multiple coupled governing equations. Historically, consideration of transport problems in two or three dimensions involving multiple interacting species has been difficult, if not impossible, on machines other than supercomputers, because of the computational time and storage required to perform such simulations. The Local Adaptive Grid Refinement method (LAGR), however, brings efficiency to such problems by determining where increased computational resolution is required in order to obtain the desired accuracy. This is done automatically and continuously during the simulation.

2 Methodology

The LAGR method is based on the initial demonstrations of *Berger and Oliger* [1984] and *Skamarock* et al. [1989]. *Berger and Oliger* [1984] present the method and solve moving shock problems. *Skamarock* et al. [1989] solve numerical weather prediction problems describing the movement of a barotropic cyclone and the evolution of a baroclinically unstable jet. For both applications, a subset of the Navier-Stokes equations is solved in order to determine velocity vectors and such scalar quantities as pressure and temperature. In this work, we build upon these initial demonstrations and develop a general system which operates independently of the governing equations, thereby allowing flexibility in the number of scalar quantities in the solution module.

The LAGR algorithm is implemented in a set of modular programs that individually perform the functions of error estimation, subgrid generation, and interface communication. The solution procedure is as follows. We begin with a coarse grid solution at some time t. The numerical errors associated with the computation on this grid are estimated and nodes for which the estimated error exceeds a specified tolerance are flagged. Then, subgrids with finer space and time discretization are fit around the flagged nodes. Initial and boundary conditions are interpolated from the coarse grid or from existing fine grids onto the new subgrids. Then each subgrid and the coarse grid are integrated independently forward in time to the next coarse grid time step at which regridding is required. The coarse grid solution is then updated with the more accurate subgrid solutions. The numerical error may also be estimated on the subgrids and still finer grids introduced.

To illustrate how this system works, consider the schematic of grid layers in Figure 1. In one coarse grid (G_O) time step, the (G_1) level grid is integrated twice and the (G_2) level grid is integrated four times, two for each (G_1) integration. The refinements in time and space do not need to be by a factor of 2 and the number of levels of refinement need not be limited to 2. There is a trade-off, however, between the refinement ratio of a subgrid and its parent grid and the number of levels that are created.

2.1 Error Estimation

The first step in the regridding process involves identifying the regions on the original grid requiring refinement. Errors on a grid are estimated with an efficient checking algorithm based on Richardson extrapolation. If the solution is smooth, the local truncation error of a finite difference method can be expressed as [*Oliger*, 1984]

$$\begin{aligned} u(x,t+k) - Q_h(u(x,t)) &= k(c_1(x,t)k^{q_1} + c_2(x,t)h^{q_2}) + kO(k^{q_1+1} + h^{q_2+1}) \\ &= \tau(x,t) + kO(k^{q_1+1} + h^{q_2+1}) \end{aligned} \tag{1}$$

where u is the dependent variable, q_1 and q_2 are the orders of accuracy in time and space, Q_h is an operator representing the finite difference scheme and defined as $\hat{u}(x,t+k) = Q_h(u(x,t))$, and $O(...)$ represents the higher order terms. Now, if two steps are taken with this method, the truncation error can be estimated as

$$u(x,t+2k) - Q_h^2(u(x,t)) = 2\tau + kO(k^{q_1+1} + h^{q_2+1}) \tag{2}$$

where Q_h^2 indicates two steps forward in time. If we take a step using the operator Q_{2h} which is the same difference operator as Q_h but with space and time steps sizes of 2h and 2k, and if $q_1 = q_2 = q$, then

$$u(x,t+2k) - Q_{2h}(u(x,t)) = 2^{q+1}\tau + kO(h^{q+1} + k^{q+1}) \tag{3}$$

Thus, an estimate of the local truncation error τ can be computed by comparing solutions on a grid of h and k discretization with solutions on a coarser grid of 2h and 2k discretization:

$$\tau = \frac{Q_h^2(u(x,t)) - Q_{2h}(u(x,t))}{2^{q+1} - 2} + O(h^{q+2}) \tag{4}$$

This method is quite general because the same solver used to integrate the equations is used to compute Q_h^2 and Q_{2h} for the error estimation in equation (4). The computations are inexpensive because no computations at the fine grid discretization are performed. Using this method, the exact form of the truncation error need not be known because the functions c_1 and c_2 in equation (1) are never calculated. Coarse grid nodes for which the estimated truncation error exceeds a prescribed tolerance are flagged in order to determine where mesh refinement is needed.

2.2 Subgrid Generation

After flagging the nodes on the base grid at which the numerical error exceeds a desired threshold, the next step is to cluster a region encompassing those nodes into a subgrid of finer discretization. The simplest method involves first clustering the nodes in groups based on proximity to one another and then fitting rectangles about the flagged nodes. If the ratio of flagged nodes to unflagged nodes within a fitted rectangle is too small, indicating an inefficient fit, the rectangle is further subdivided until the ratio is acceptable. After the clusters of flagged nodes have been divided into efficient groups, a buffer zone between the flagged nodes and the subgrid boundary is provided. Doing so insures that the boundaries of the subgrid are not placed in a region of high error. The size of the buffer zone also helps determine how frequently the regridding process must occur. The larger the buffer zone, the less frequently regridding must be performed. Supplying a large buffer, however, results in less efficient subgrids.

Once a subgrid with finer space and time discretization has been created, the next step is to establish the initial and boundary conditions. These are interpolated from either the coarse grid

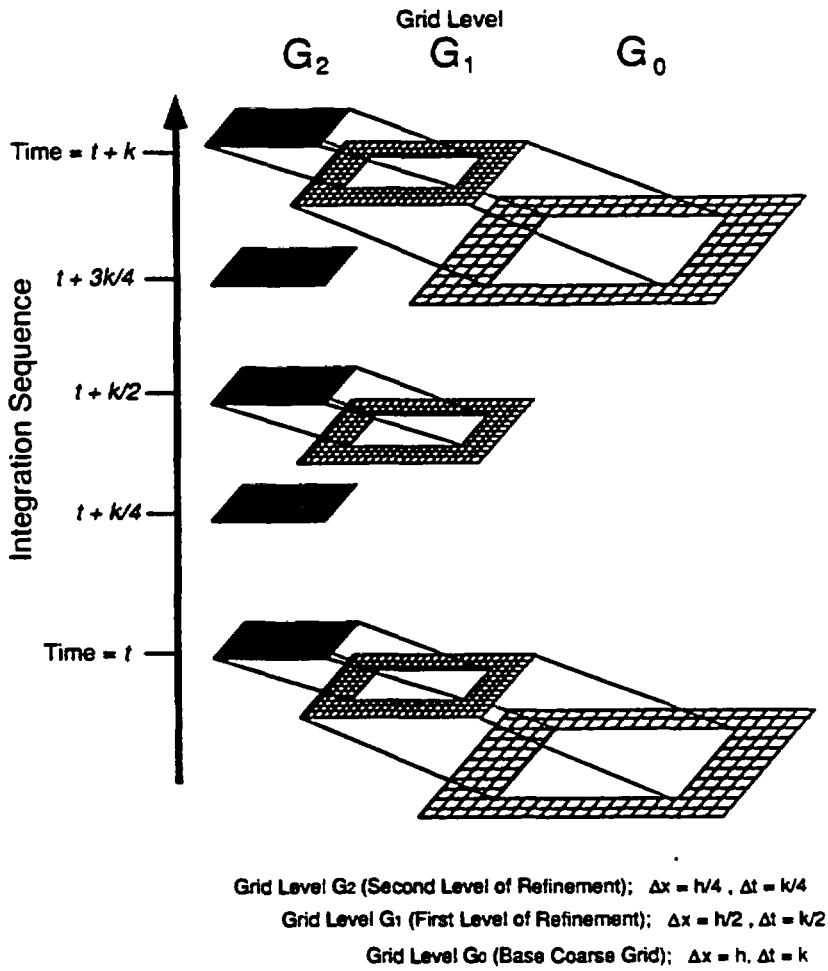

Figure 1: Integration over one coarse grid time step with LAGR. System has two levels of refinement and refinement ratios of 0.5 in time and space.

or from previously existing fine grids. At this point the subgrid is an independent unit which is advanced forward in time to the next coarse grid time step, at which point the solution on the high resolution subgrid is used to update the solution on the coarse grid.

2.3 Data Structure and Grid Management

Information storage and transfer for this method are maintained by a data structure which stores two kinds of information: descriptions of the grids and the grid solution vectors. All solution vectors are stored in one array. This array is managed as a linked list of used and available blocks of storage. The management routines maintain the data structure, implement the grid communication routines, and advance the solutions on the various grids at the various levels in the appropriate sequence.

2.4 Implementation of LAGR for Solute Transport Problems

In this paper we use the following common partial differential equation to describe the mass balance in a groundwater solute transport system:

$$\theta \frac{\partial \tilde{c}_i}{\partial t} = \nabla \cdot (\mathbf{D} \nabla \tilde{c}_i - \mathbf{v} \tilde{c}_i) + q \qquad i = 1, 2, ..., N_{\tilde{c}} \tag{5}$$

where θ is the porosity, t is time, ∇ is the gradient operator, D is the dispersion tensor, v is the seepage velocity, q is a source term, and $\tilde{c}_i$ is the concentration of component i. The components are defined such that their global mass is reaction invariant. Thus, they are equivalent to tenads as defined by *Rubin* [1983]. When the grid Peclet number, Pe_g, defined as $\mathbf{v}\Delta\mathbf{x}/\mathbf{D}$, is large, standard uniform grid methods are inefficient because of the fine discretization required to achieve accurate results. For non-reactive, single species problems, the species concentration is equivalent to the component concentration and equation (5) is the common advection-dispersion equation. This equation is often used to benchmark alternative numerical methods which strive for accurate numerical solutions when Pe_g is large [*Ahlstrom* et al., 1977; *O'Neill*, 1981; *Thompson* et al., 1984; *Neuman*, 1984; *Elnawawy* et al., 1990; and *Yeh*, 1990].

When multiple, reactive species are present, equation (5) represents a system of coupled equations. For demonstration purposes, we choose a competitive sorption problem where the chemical process involves multiple cations in solution competing for exchange sites on the aquifer material. In Figure 2, we show a cartoon of the ion-exchange process that takes place at the pore scale. The two invader ions, species 2 and species 3, move into a system where species 1 is at equilibrium between its aqueous and sorbed phases. As the two invader cations move in, they preferentially displace the sorbed phase of cation 1.

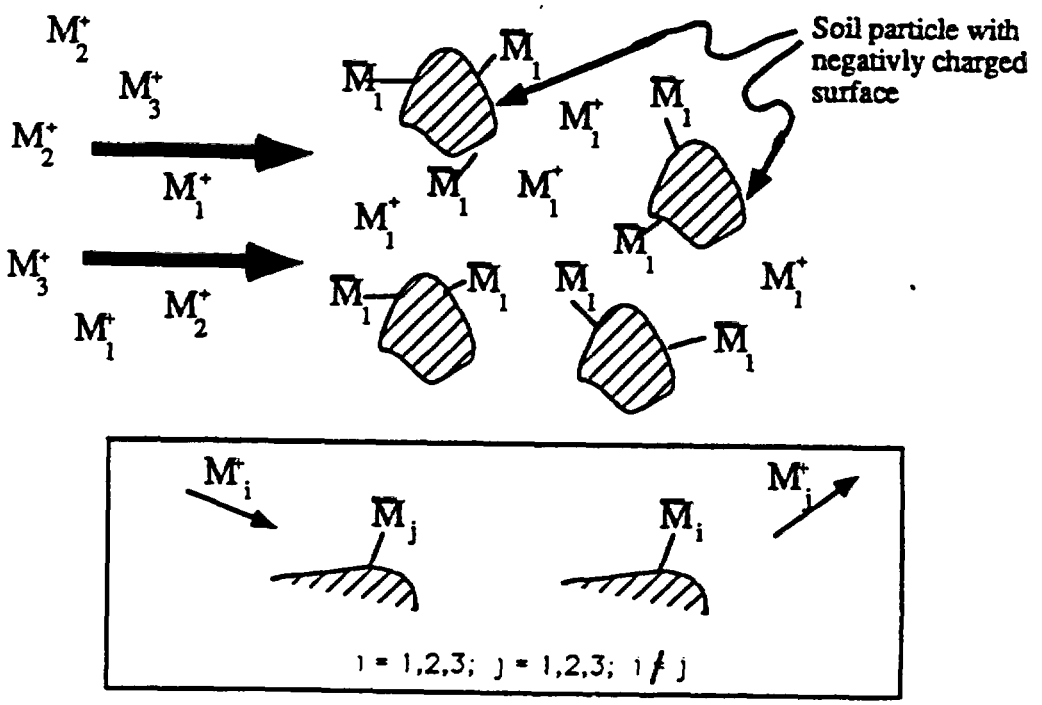

Figure 2: Pore scale ion-exchange process

Cation 3 sorbs more readily than cation 2 which in turn sorbs more readily than the resident cation 1. When sorption/desorption processes are involved, equation (5) takes the following form:

$$\frac{\partial c_i}{\partial t} + \frac{\partial \bar{c}_i}{\partial t} = \nabla \cdot (\mathbf{D}\nabla c_i - \mathbf{v}c_i) \quad i = 1,2,3 \tag{6}$$

where c_i is the aqueous concentration of cation i and $\bar{c}_i$ is sorbed phase concentration of cation i. The coupling for this system of equations comes from the algebraic equations which describe the equilibrium reactions:

$$M_3 + \overline{M_1 M_s} \rightleftharpoons M_1 + \overline{M_3 M_s}\,; \quad K_{31} = \frac{c_1 \bar{c}_3}{\bar{c}_1 c_3} \tag{7}$$

$$M_2 + \overline{M_1 M_s} \rightleftharpoons M_1 + \overline{M_2 M_s}\,; \quad K_{21} = \frac{c_1 \bar{c}_2}{\bar{c}_1 c_2} \tag{8}$$

where M_i indicates an aqueous ion, $\overline{M_i M_s}$ indicates an ion in the sorbed phase, and K_{ij} is the equilibrium coefficient which describes the partitioning between the sorbed and aqueous phases for species i and j. From these equations, the following equilibrium partitioning between M_3 and M_2 is derived:

$$M_3 + \overline{M_2 M_s} \rightleftharpoons M_2 + \overline{M_3 M_s}\,; \quad K_{32} = \frac{c_3 \bar{c}_2}{\bar{c}_3 c_2} = \frac{K_{31}}{K_{21}} \tag{9}$$

One solution technique for this problem is described in detail in section 4 of *Rubin* [1990]. A particularly attractive aspect of Rubin's method is that the $\frac{\partial \bar{c}_i}{\partial t}$ terms are replaced with c_i, $\bar{c}_i$, and $\frac{\partial c_i}{\partial t}$ terms thereby reducing the non-linearity of the system. Starting with the basic governing equation (6), Rubin's derivation yields the following operational equation set for this problem:

$$\frac{\partial c_1}{\partial t} + \frac{[\bar{c}_2 + \bar{c}_3] - \bar{c}_1[K_{21}\frac{\partial c_2}{\partial t} + K_{31}\frac{\partial c_3}{\partial t}]}{c_1 + K_{21}c_2 + K_{31}c_3} = \nabla \cdot (\mathbf{D}\nabla c_1 - \mathbf{v}c_1) \tag{10}$$

$$\frac{\partial c_2}{\partial t} + \frac{[\bar{c}_1 + \bar{c}_3] - \bar{c}_2[K_{12}\frac{\partial c_1}{\partial t} + K_{32}\frac{\partial c_3}{\partial t}]}{c_2 + K_{12}c_1 + K_{32}c_3} = \nabla \cdot (\mathbf{D}\nabla c_2 - \mathbf{v}c_2) \tag{11}$$

$$\frac{\partial c_3}{\partial t} + \frac{[\bar{c}_1 + \bar{c}_2] - \bar{c}_3[K_{13}\frac{\partial c_1}{\partial t} + K_{23}\frac{\partial c_2}{\partial t}]}{c_3 + K_{13}c_1 + K_{23}c_2} = \nabla \cdot (\mathbf{D}\nabla c_3 - \mathbf{v}c_3) \tag{12}$$

where

$$\bar{c}_1 = \bar{c}_T / [1 + K_{12}c_2/c_1 + K_{13}c_3/c_1] \tag{13}$$

$$\bar{c}_2 = K_{12}\bar{c}_1 c_2/c_1 \tag{14}$$

$$\bar{c}_3 = K_{13}\bar{c}_1 c_3/c_1 \tag{15}$$

$$\bar{c}_T = \text{The exchange capacity of the aquifer material} \tag{16}$$

This operational set of equations comprise a system of coupled, quasi-linear PDE's. For this problem, they are solved using a predictor-corrector method. When more chemical processes are included in the problem description, such as aqueous complexation and/or oxidation/reduction processes, the resulting system of operational equations may be highly nonlinear, thereby necessitating iterative methods such as Picard iteration or Newton-Raphson iteration.

3 Results/Applications

In this section we present results which demonstrate how LAGR obtains accuracy equivalent to uniform fine grid computations at a fraction of the computational cost. We first present solutions to benchmark problems which have been cited in the literature as test cases for numerical approximations of single component, non-reactive, advection-dispersion problems. Then, we present results for a reactive multicomponent problem in order to demonstrate LAGR's ability to handle complex problem formulations as well. For these examples, we compare results computed on a uniform coarse grid, a uniform fine grid, with LAGR, and when available, with analytical approximations. All of our computations are performed using a QUICK finite difference spatial discretization [*Leonard*, 1979] and either a Crank-Nicholson time step for the single component problems or a hybrid Runge-Kutta predictor-corrector time step for the multicomponent problems. The cost and accuracy of the simulations are summarized in the tables for each example. The cost is reported in CPU units on the IRIS 4D/380GTX Power Series computer. Preliminary results indicate that similar relative performance measures are obtained on other workstations as well. The accuracy is reported as the root mean square error (RMSE) defined as:

$$\text{RMSE} = \frac{\sqrt{\sum(a(i) - n(i))}}{\text{N}} \tag{17}$$

where *a(i)* is the analytical solution at node *i*, *n(i)* is the numerical approximation at node *i* and N is the number of nodes in the computational domain. For problems with no analytical solution, a relative RMSE is computed using the solution on the finest uniform grid as an approximation of *a(i)*.

3.1 Single Species Problem 1

Problem 1 concerns the advancement of a plume from a constant source in a two-dimensional domain. Figure 3 shows the domain and initial conditions for this problem. This setup has been used by *Elnawawy* et al. [1990] and *Daus and Frind* [1985] and the analytical solution is given by *Cleary* [1979]. Equation (5) is the governing equation. We document two runs with isotropic dispersivities to show the effect of increasing the grid Peclet number. In the first run, both D_x and D_y are equal to 0.1 and in the second run, they are both equal to 0.01. The groundwater velocity in the x direction is 0.125 m/day and the porosity is 0.25. As the coarse grid node spacing is 2 meters in both the x and y direction and the time step is 1 day, the grid Peclet numbers for the two runs are 2.5 and 25, respectively. The results for these conditions are plotted in Figure 4. For a grid Peclet number of 2.5, the coarse grid performs well. However, for a grid Peclet number of 25, oscillations plague the solution. The numerical errors are overcome when LAGR is used because the grid Peclet number is reduced locally to 6.25 as the grid spacing is reduced locally to 0.5 meters. The Courant number remains unchanged because the ratio of space to time discretizations remains constant. Figure 5 shows where the subgrids are placed as the front moves through the domain. Table 1 sumarizes the performance and cost of these simulations.

3.2 Single Species Problem 2

In this second problem involving the single species advection-dispersion equation, we consider an initial pulse which travels in a direction rotated 45° from the x axis. This problem tests a numerical method's ability to overcome "grid orientation error" caused by the deviation of flow lines from the grid lines [*Elnawawy* et al., 1990]. Here, we introduce a pulse based on a normal distribution of

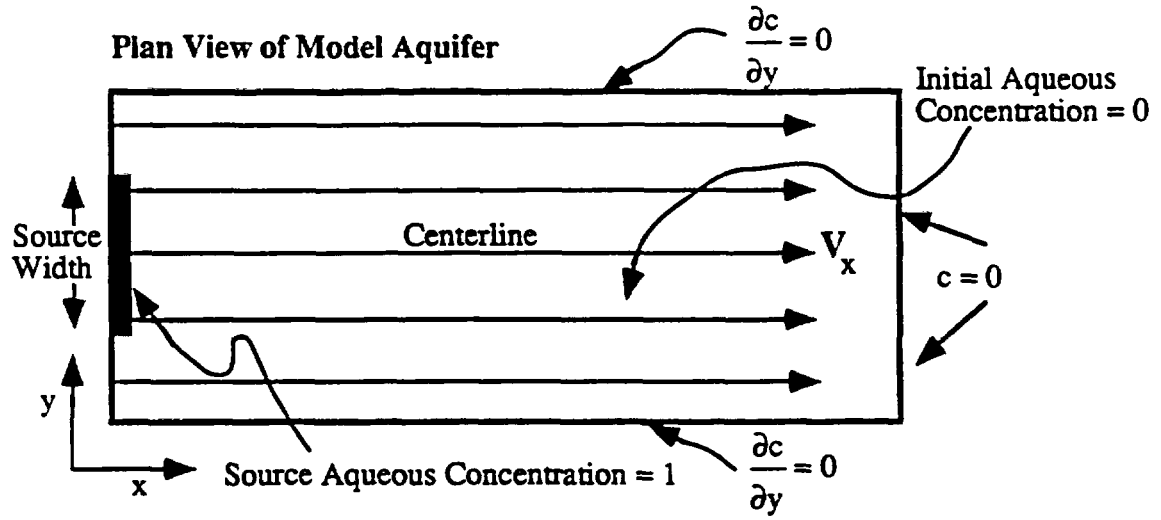

Figure 3: Domain, initial conditions, and boundary conditions for Problem 1

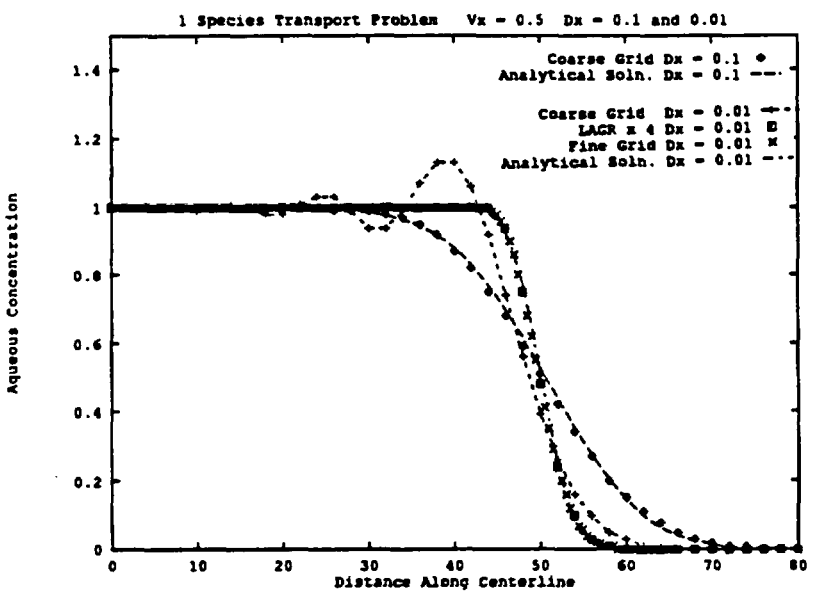

Figure 4: Comparison of coarse grid, fine grid, and LAGR solutions along centerline at time = 100. When $D_x = 0.1$, $Pe_g(coarse) = 2.5$ and $Pe_g(fine) = 0.625$. When $D_x = 0.01$, $Pe_g(coarse) = 25$ and $Pe_g(fine) = 6.25$.

Table 1: Results for Example Problem 1

Method	RMS Error	CPU	%Fine CPU
Fine	6.5×10^{-4}	416	100
Coarse	7.8×10^{-1}	5	1
LAGR	4.6×10^{-4}	85	21

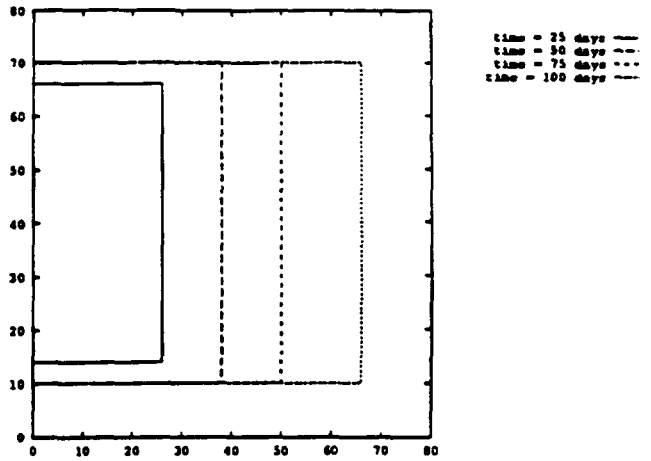

Figure 5: Subgrid placement at time = 25, 50, 75, and 100 days for Problem 1

concentration and allow it to be transported through the solution domain. The solutions after 150 days of simulated time are then compared to the well known analytical solution for this problem. The examples shown are computed using a velocity field diagonal to the x axis with a magnitude of 0.42 m/d and dispersivities in both directions of 0.04 m. Figure 6 shows the propagation of the subgrid for this problem. The solutions for computations using a uniform coarse grid, a uniform fine grid (4 times finer in space and time discretization) and LAGR are compared with the analytical solution in Figure 7 and the results are compared in Table 2.

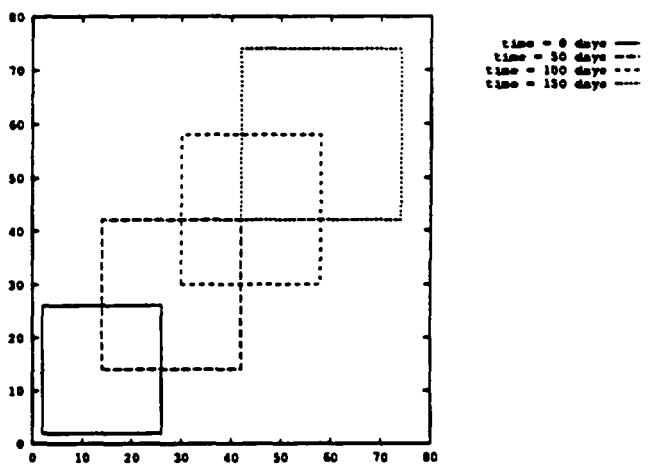

Figure 6: Example Subgrid placement at time = 0, 50, 100, and 150 days for Problem 2

3.3 Multicomponent Problem

In this example problem we demonstrate the portability of LAGR from the simple single species problems in the first two examples to a complex problem involving multiple, reacting species. The equation set which governs this transport process involves a system of coupled, nonlinear equations which describe the transport and chemical interactions of the various species. For this example involving competitive ion-exchange between 3 species, equations 10 through 15 describe

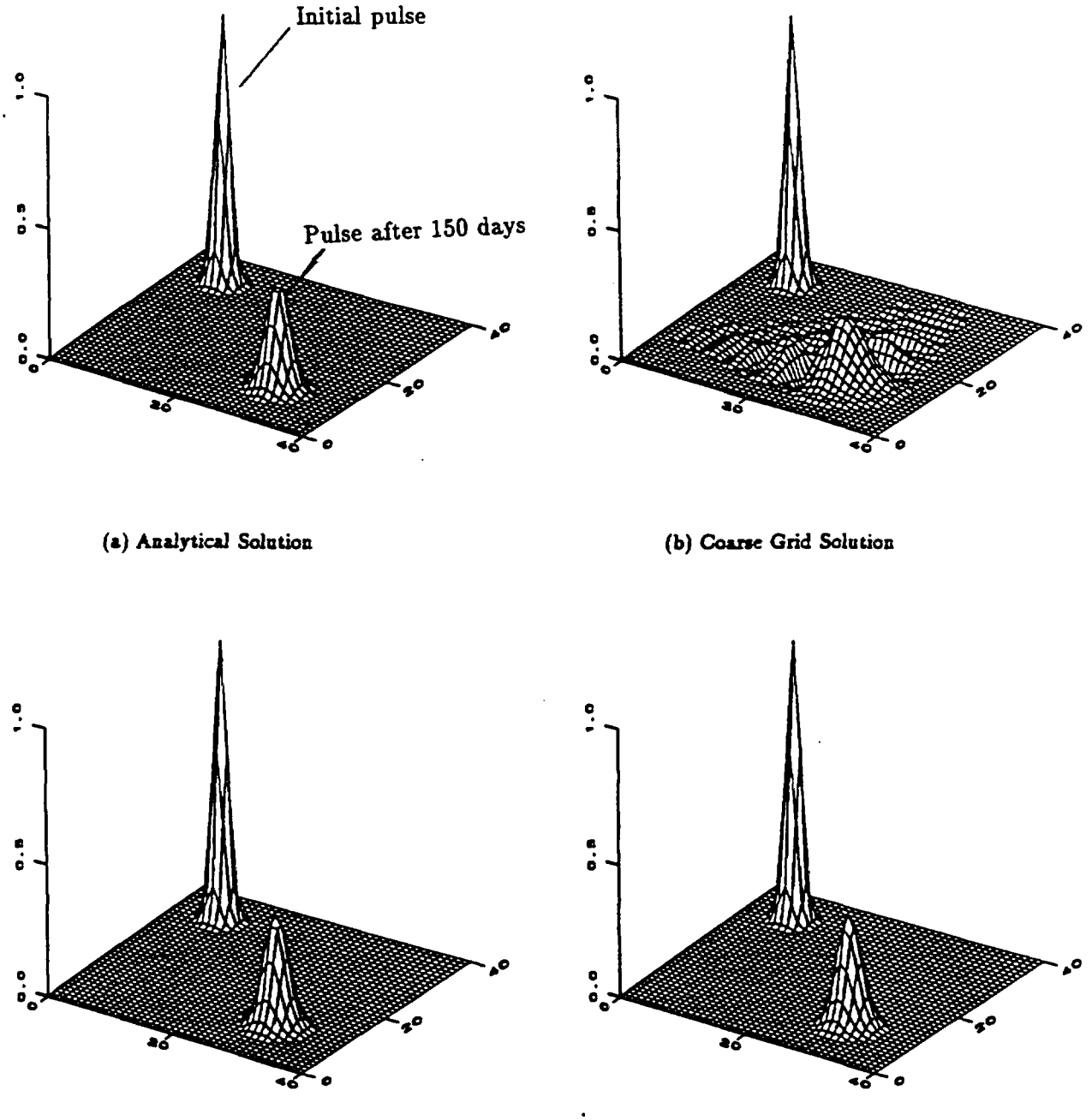

(a) Analytical Solution

(b) Coarse Grid Solution

(c) Fine Grid Solution

(d) LAGR Solution

Figure 7: Example Problem 2 Results at time t = 150 days. Fine grid is 4X finer than coarse grid in both space and time. All results shown at coarse grid discretization.

Table 2: Results for Example Problem 2

Method	RMS Error	CPU	%Fine CPU
Fine	2.5×10^{-3}	511	100
Coarse	2.4×10^{-2}	7	1
LAGR	3.1×10^{-3}	93	18

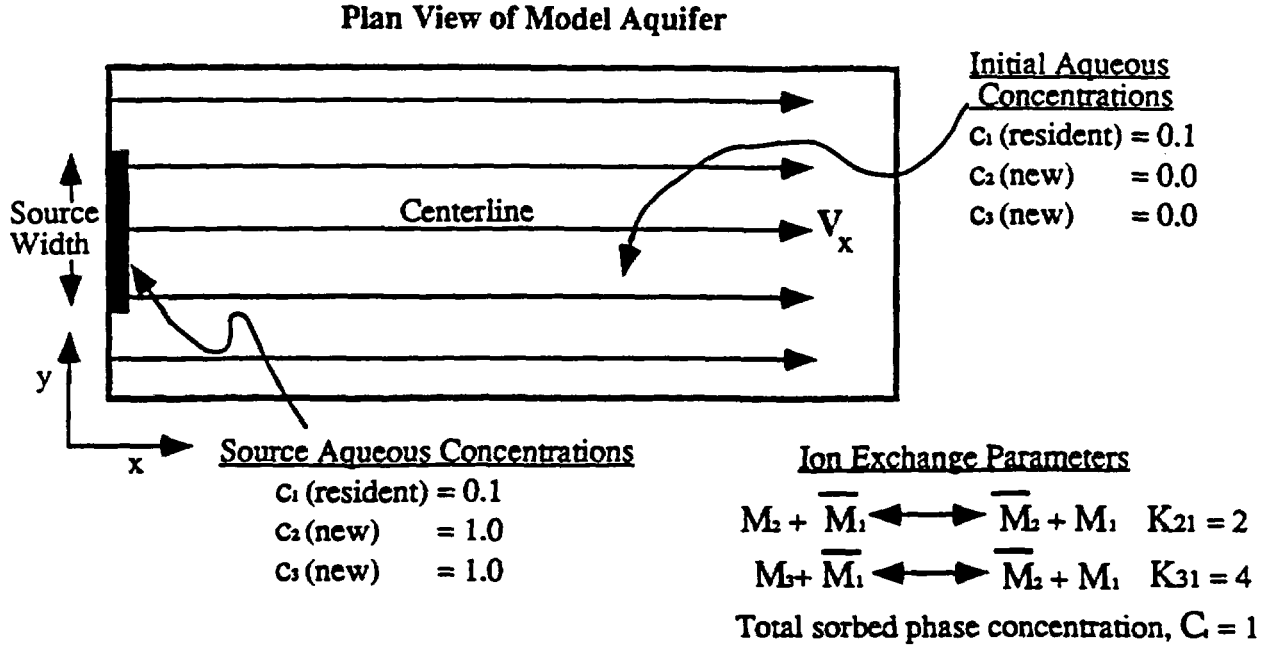

Figure 8: Domain, initial conditions, and boundary conditions for Problem 3

the processes involved. The conversion from the single species problems to this more complicated problem involves merely supplying a routine that can solve this system of equations to obtain c_1, c_2, and c_3. The method of solution is inconsequential to the LAGR routines. All of the grid management routines remain intact. The problem domain and initial and boundary conditions are given in Figure 8. Figure 9 shows the resulting two-dimensional plumes of the aqueous phases that result in this problem. As a result of the preferential sorption by the invader species (M_2 and M_3), the trailing edge of the species 1 plume and the leading edge of the species 2 plume experience "self sharpening" [*Valocchi* et al., 1981]. These sharp fronts require even greater numerical resolution than a non-reactive species front requires for similar transport conditions. Although we have no analytical solution with which to compare our results, a comparison of the solutions obtained using a uniform coarse grid, a uniform fine grid, and LAGR (see Figure 10) indicates the accuracy that is lost if sufficient resolution is not supplied. Table 3 shows the accuracy and computational cost for the three solutions for this problem.

Table 3: Results for Example Problem 3

Method	RMS Error[a]	CPU	%Fine CPU
Fine		4188	100
Coarse	2.3×10^{-1}	130	1
LAGR	1.2×10^{-6}	813	19

[a] Relative to fine grid solution

4 Conclusion

The local adaptive grid refinement (LAGR) method effectively brings efficiency to accurate solutions of complex solute transport problems. By refining only the regions where increased discretization is needed, unnecessary computations are avoided elsewhere in the domain. These refinements are provided continuously and automatically throughout the simulation.

In order to demonstrate the efficiency and accuracy afforded by LAGR, we first demonstrated two problems involving the solution of the advection-dispersion equation in two spatial dimensions. In both examples, we started with a uniform coarse grid. The solutions on these grids, although inexpensive to obtain, were unacceptable due to numerical error. In the first example the numerical error is mainly attributed to the high Peclet number and in the second example to grid orientation error. Using LAGR, we were able to produce accurate solutions for these problems at a fraction of the cost of using a uniform fine grid over the entire solution domain.

We next incorporated a transport model involving three reactive species. Executing this model with LAGR involved little more than setting the number of solution variables in the LAGR data structure. It is for problems even more complex than this third example that we feel LAGR will be most useful. Consider the computational burden presented by this relatively simple multicomponent problem. The solution domain and initial conditions are similar to those of the first single component problem. However, computing solutions for the multicomponent problem requires approximately ten times more CPU time than is required for the single component problem. As the complexity of the multicomponent problem increases, this ratio will also increase. Thus LAGR should be instrumental in solving problems which would otherwise be too large and take too long.

Acknowledgments

The research on which this report is based was financed in part by the United States Department of the Interior, Geological Survey, through the State Water Resources Research Institute, Project No. 14-08-0001-61550, and by the University of California Water Resources Center, Project UCAL-WRC-W-737. Contents of this publication do not necessarily reflect the views and policies of the U.S. Department of the Interior, nor does mention of trade names or commercial products constitute their endorsement or recommendation for use by the U.S. Government. The authors would like to acknowledge the assistance provided by Prof. Joe Oliger in making many of the original adaptive grid codes available.

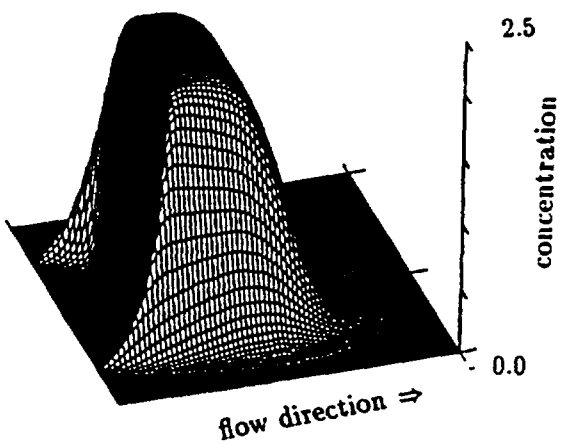

(a) Species 1

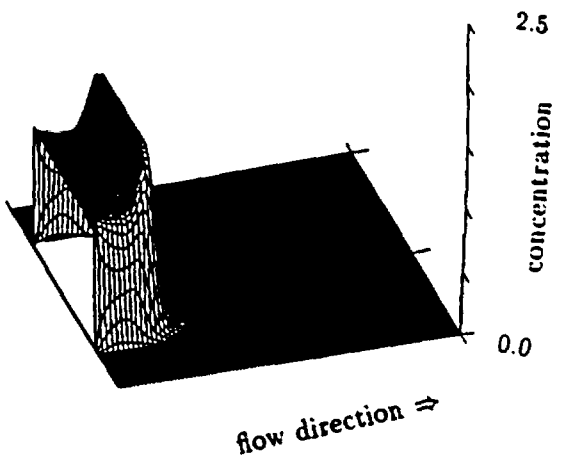

(b) Species 2

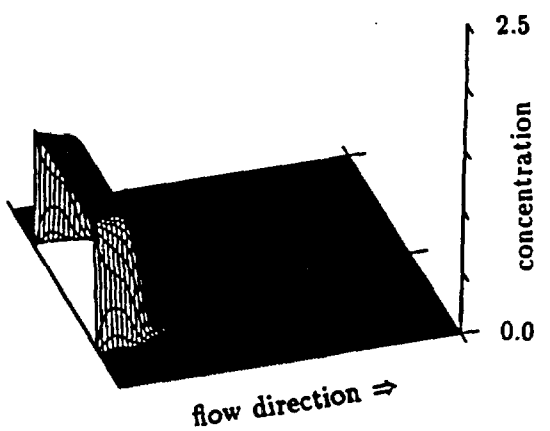

(c) Species 3

Figure 9: Plumes of the three aqueous species at time = 100.

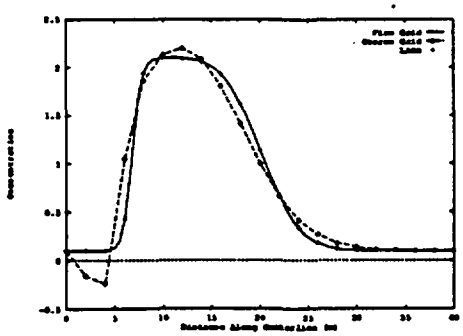

(a) Species 1

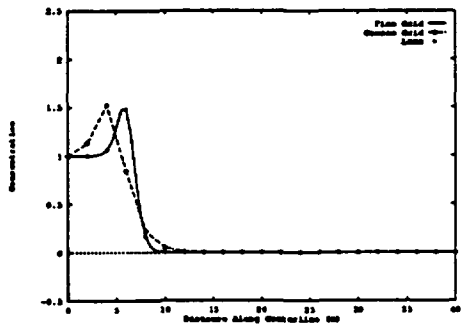

(b) Species 2

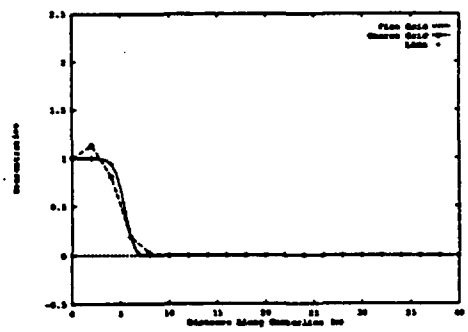

(c) Species 3

Figure 10: Centerline concentrations of the three aqueous species at time = 100

References

[Ahlstrom *et al.*, 1977] S.W. Ahlstrom, H.P. Foote, R.C. Arnett, C.R. Cole, and R.J Sene. Multicomponent mass transport model: Theory and numerical implementation (discrete-parcel-random-walk version). Technical Report BNWL-2127/UC-70/UC-32, Battelle Pacific Northwest Laboratories, 1977.

[Berger and Oliger, 1984] M.J. Berger and J.O. Oliger. Adaptive mesh refinement for hyperbolic partial differential equations. *Jnl. Comp. Phys.*, 53:484–512, 1984.

[Cleary, 1979] R.W. Cleary. Analytical models for groundwater pollution and hydrology. Technical Report 78-WR-15, Dept. of Civ. Eng., Princeton Univ., Princeton, N.J., 1979.

[Daus and Frind, 1985] A.D. Daus and E.O. Frind. An alternating direction galerkin technique for simulation of contaminant transport in complex groundwater systems. *Water Resources Research*, 21(5):653–664, 1985.

[Elnawawy *et al.*, 1990] O.A. Elnawawy, A.J. Valocchi, and A.M. Ougouag. The cell analytical-numerical method for solution of the advection-dispersion equation: Two-dimensional problems. *Water Resources Research*, 26(11):2705–2716, 1990.

[Leonard, 1979] B.P. Leonard. A stable and accurate modelling procedure based on quadratic upstream modelling. *Comput. Methods Appl. Mech. Engr.*, 19:59–98, 1979.

[Neuman, 1984] S.P. Neuman. Adaptive Eulerian-Lagrangian finite element method for advection-dispersion. *Intl. Jnl. For Numerical Methods in Engineering*, 20:309–323, 1984.

[Oliger, 1984] J.O. Oliger. Adaptive grid methods for hyperbolic partial differential equations. *Inverse Problems of Acoustic and Elastic Waves*, pages 320–331, 1984.

[O'Neill, 1981] K. O'Neill. Highly efficient, oscillation free solution of the transport equation over long times and large spaces. *Water Resources Research*, 17(6):327–339, 1981.

[Rubin, 1983] J. Rubin. Transport of reacting solutes in porous media: Relation between mathematical nature of problem formulations and chemical nature of reactions. *Water Resources Research*, 19(5):1231–1252, 1983.

[Rubin, 1990] J. Rubin. Solute transport with multisegment, equilibrium-controlled reactions: A feed forward simulation method. *Water Resources Research*, 26(9):2029–2055, 1990.

[Skamarock *et al.*, 1989] W.C Skamarock, J.O. Oliger, and R.L. Street. Adaptive grid refinement for numerical weather prediction. *Jnl. Comp. Phys.*, 80:27–60, 1989.

[Thompson *et al.*, 1984] N.R. Thompson, J.F. Sykes, and W.C. Lennox. A Lagrangian porous media mass transport model. *Water Resources Research*, 20(3):391–399, 1984.

[Valocchi *et al.*, 1981] A.J. Valocchi, R.L. Street, and P.V. Roberts. Transport of ion-exchanging solutes in groundwater: Chromatographic theory and field simulation. *Water Resources Research*, 17(5):1517–1527, 1981.

[Yeh, 1990] G.T. Yeh. A Lagrangian-Eulerian method with zoomable hidden fine-mesh approach to solving advection-dispersion equations. *Water Resources Research*, 26(6):1133–1144, 1990.